

FEATURES PRESERVING CONTRAST IMPROVEMENT FOR RETINAL VASCULAR IMAGES

QAISAR ABBAS^{1,2}, AMJAD FAROOQ^{1,2}, M. TAHIR ABBAS KHAN³
M. EMRE CELEBI⁴, IRENE FONDÓN GARCÍA⁵
S. JIMÉNEZ CARMONA⁶ AND PEDRO ALEMANY⁶

¹Department of Computer Science

²Centre for Imaging and Computational Intelligence
COMSATS Institute of Information Technology Sahiwal Campus
COMSATS Road, Off G.T. Road, Sahiwal, Pakistan
{ drqaisar; amjadfarooq }@ciitsahiwal.edu.pk

³Ritsumeikan Asia Pacific University
1-1 Jumonjibaru, Beppu-shi, Oita 874-8577, Japan

⁴Department of Computer Science
Louisiana State University
Shreveport, LA, USA

⁵Department of Signal Theory and Communications
School of Engineering Path of Discovery
s/n C.P. 41092, Seville, Spain

⁶Servicio Andaluz de Salud
Cádiz, Spain

Received February 2012; revised December 2012

ABSTRACT. *Retinal vascular images are widely used to diagnose the retina-related visual impairment and blindness caused by diabetic retinopathy. These images often have low contrast and uneven illumination due to acquisition procedure, which can affect diagnosis process. This paper presents a novel color contrast enhancement method that preserves the features of the images using multiscale discrete-shearlet transform (DST), the perceptual uniform color space CIEL*a*b* and incorporating local-influence control function. The developed method is compared with state-of-the-art methods by using PSNR image quality measure. The applicability of this method has been tested on total 271 retinal images obtained from two publicly available datasets DRIVE, STARE and another private one provided by medical experts from the Hospital Puerta del Mar (Cádiz, Spain). The comparative results indicate that our enhancement method outperforms.*

Keywords: Diabetic retinopathy, Retinal image enhancement, Vascular-network segmentation, Discrete shearlet transform

1. Introduction. Glaucoma, Diabetic retinopathy and age-related macular degeneration are diseases that cause retina-related visual impairment and blindness worldwide. For instance, in the U.S., 937,000 people were blind in 2002 and 2.4 million people had visual problems [1]. For early and routine diagnoses, the ophthalmologists [2] widely use image analysis tools trying to make use of non-invasive acquisition techniques to visualize the human retina. Nowadays, there are some automatic screening tools developed [3-9] to investigate diabetic retinopathy (DR) trying to identify some features among others as the vascular blood vessels, fovea and optic disc (OD).

As retinal vascular images are captured with digital fundus cameras, the uneven light illumination, surrounding conditions and acquisition process irremediably affect image

quality. Therefore, an improvement is always required to enhance the light and contrast across the image.

To enhance the visual quality of these images, there are a few methods [10-14] in the literature. The HSI (hue, saturation and intensity) based color model was used in [10] to enhance the retinal images by using the mean along with standard deviation for local contrast adjustment. In [11], a color remapping technique is proposed. This method tries to enhance luminosity and contrast on each color plane of RGB color space, independently. The Contourlet transform (CT) method was also used to enhance the retinal images in [12]. For that purpose, they used the luminance component (L^*) of CIEL*a*b* color space to enhance contrast by using a nonlinear enhancement function for each of the coefficients of the CT analysis and then, reconstructing the image by combining all these enhance coefficients. This study does not consider the uneven illumination and the noise generated in the reconstruction process. In [13], the hue, saturation and value (HSV) color space was used to provide better to decouple the chromaticity and luminance information. Unfortunately it does not preserve the fidelity of the retinal images. In [14], retinal enhancement algorithm was proposed based on image geometry. Histogram equalization (HE) is being widely utilized for both color and grayscale image enhancement. Particularly, in [15] the MMBEDHE method was developed to enhance contrast while attaining the maximum brightness. However, HE performs fine in the case of grayscale images generating unnecessary visual deterioration, including a saturation effect, when dealing with color images.

In the light of this literature review, it seems that a great effort has been done in the field enhancing the contrast of blood vessels while reducing the contrast of the bright OD and tiny dark objects like the macular area. A number of automated algorithms are being developed for the detection of red lesions (micro aneurisms and hemorrhages) as well as white lesions (exudates and cotton-like spots), but few studies focus on enhancing the quality of image, without generating extra noise.

In this paper, a retinal image enhancement solution is presented with features preserving capabilities, based on the discrete shearlet transform (DST) [16,17] in the CIEL*a*b* uniform color space and by developing a local-influence control function without generating artifacts and avoiding an excessive saturation, something that occurs in many of the state-of-the-art enhancement techniques. Nowadays, DST transform [18] is used for image enhancement because it is effective applicability in the field of image denoising. The proposed algorithm is evaluated based on three datasets, two of them publicly available, i.e., STARE [19], DRIVE [20] and one private dataset from the Hospital Puerta del Mar (Cádiz, Spain). In fact, we present (1) an enhancement method on a single color plane; (2) a solution for color image enhancement which combines a linear color remapping technique; and (3) use the local information of OD and CUP area to avoid saturation effect by local-influence correction.

2. System Architecture. The systematic flow diagram of the proposed scheme is illustrated in Figure 1. First, the retinal color images captured with the retinography are transformed from RGB to CIEL*a*b* uniform color space. The luminance (L^*) plane is decomposed by DST into different levels with the corresponding coefficients. Next, a non-linear mapping function and gamma correction methods are applied to each of the obtained coefficients for contrast enhancement. Subsequently, the inverse transform is performed with these enhanced coefficients to reconstruct the final enhanced image by combing the three planes.

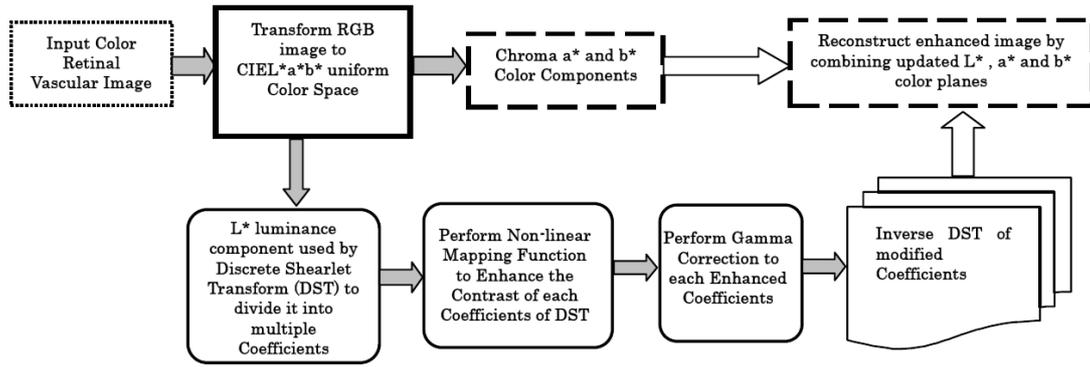


FIGURE 1. Systematic flow diagram of the proposed retinal vascular image enhancement method

2.1. Retinal image datasets. The features preserving image enhancement technique has been tested on three data sets. Two of them are available online: DRIVE [19] and STARE [20]. The third one was provided by medical experts of the Hospital Puerta del Mar (Cádiz, Spain). The DRIVE dataset was built by Netherlands to automate diabetic retinopathy system. To our purpose, 40 images have been selected from it. In this dataset, the size of each image is 768 by 584 pixels. The images in this dataset clearly contain uneven illumination and low contrast. The STARE images and their clinical data have been provided by the Shiley Eye Center at the University of California and the Veterans Administration Medical center in San Diego. We have selected among all the available images those with the poorer contrast: 81 images from this dataset to test the performance of the proposed enhancement algorithm in total. In the STARE dataset, the images are of 700×605 pixels, with 24-bis per pixel. The private dataset is compounded by images selected from the early detection of diabetic retinopathy program of the Junta de Andalucía. It includes 150 images of 50 patients and each patient eye has 3 images of 450. The resolution level is 20468×1536 and they have been stored in jpeg format.

3. Color Space Transform. The images can be represented in many color spaces (RGB, HSV, etc.) and the selection of one of them highly depends on the application. In this case, the enhancement algorithm has been designed to help physicians in their task of early diagnose of retinopathy and therefore the selected space must be as close as possible to human perception. In the past studies, the CIE L*a*b* and CIE L*u*v* are two color spaces, which are used for human perception. Although, both of them have been widely used, the white adaptation in CIE L*u*v* (with a subtractive change that involves a vectorial displacement instead of the multiplicative normalization that will produce the desired proportional movement) can occasionally lead to poorer results. Therefore, the proposed algorithm initially transforms the fundus images from sRGB color space to CIE L*a*b* color space [21].

The CIE L*a*b* color space, introduced by CIE in 1976, was designed specifically to be uniform, that is Euclidean distances between two colors represented in this space needed to be related to de perceived distance between them, achieving high correlation with human perception. This color space also takes into account chromatic adaptation and the non-linearity of human visual response [22]. The equations that relate the coordinates in this space with the tristimuli XYZ are:

$$L^* = \left\{ \begin{array}{ll} 116 \left(3 \sqrt{\frac{Y}{Y_n}} \right) - 16 & \text{if } si \left(\frac{Y}{Y_n} \right) > 0.01 \\ 903.3 \left(\frac{Y}{Y_n} \right) & \text{if } si \left(\frac{Y}{Y_n} \right) < 0.01 \end{array} \right\}$$

$$\begin{aligned} a^* &= 500 \left(\left(\frac{X}{X_n} \right)^{1/3} - \left(\frac{Y}{Y_n} \right)^{1/3} \right) \\ b^* &= 200 \left(\left(\frac{Y}{Y_n} \right)^{1/3} - \left(\frac{Z}{Z_n} \right)^{1/3} \right) \end{aligned} \quad (1)$$

where, X_n , Y_n and Z_n are the corresponding values of the reference white.

L^* plane represents lightness with values ranging from 0 (black) and 100 (white) if X , Y , and Z are between 0 and 1. a^* and b^* represent opponent color scales red-green and blue-yellow respectively. Original images are firstly transformed from *sRGB* to *CIE XYZ* color space by Equation (2), and subsequently expressed in $CIE L^*a^*b^*$ color space by means of Equation (2).

$$\begin{pmatrix} X \\ Y \\ Z \end{pmatrix} = \begin{pmatrix} 0.4124 & 0.3576 & 0.1805 \\ 0.2126 & 0.7152 & 0.0722 \\ 0.0193 & 0.1192 & 0.9505 \end{pmatrix} \begin{pmatrix} R \\ G \\ B \end{pmatrix} \quad (2)$$

An example of an image from DRIVE dataset, which is transformed to each plane of $CIE L^*a^*b^*$ color space is visually represented in Figure 2(a), Figure 2(b) and Figure 2(c), respectively. In this figure, the x-axis represents distance along the line and the y-axis is the pixel intensity. It should be noticed from this figure that the plots are having different intensities values with different distance and therefore a linear contrast enhancement solution may not be an appropriate choice for retinal image contrast enhancement. Moreover, the luminance image (L^*) of $CIE L^*a^*b^*$ color space is having highest smooth distances

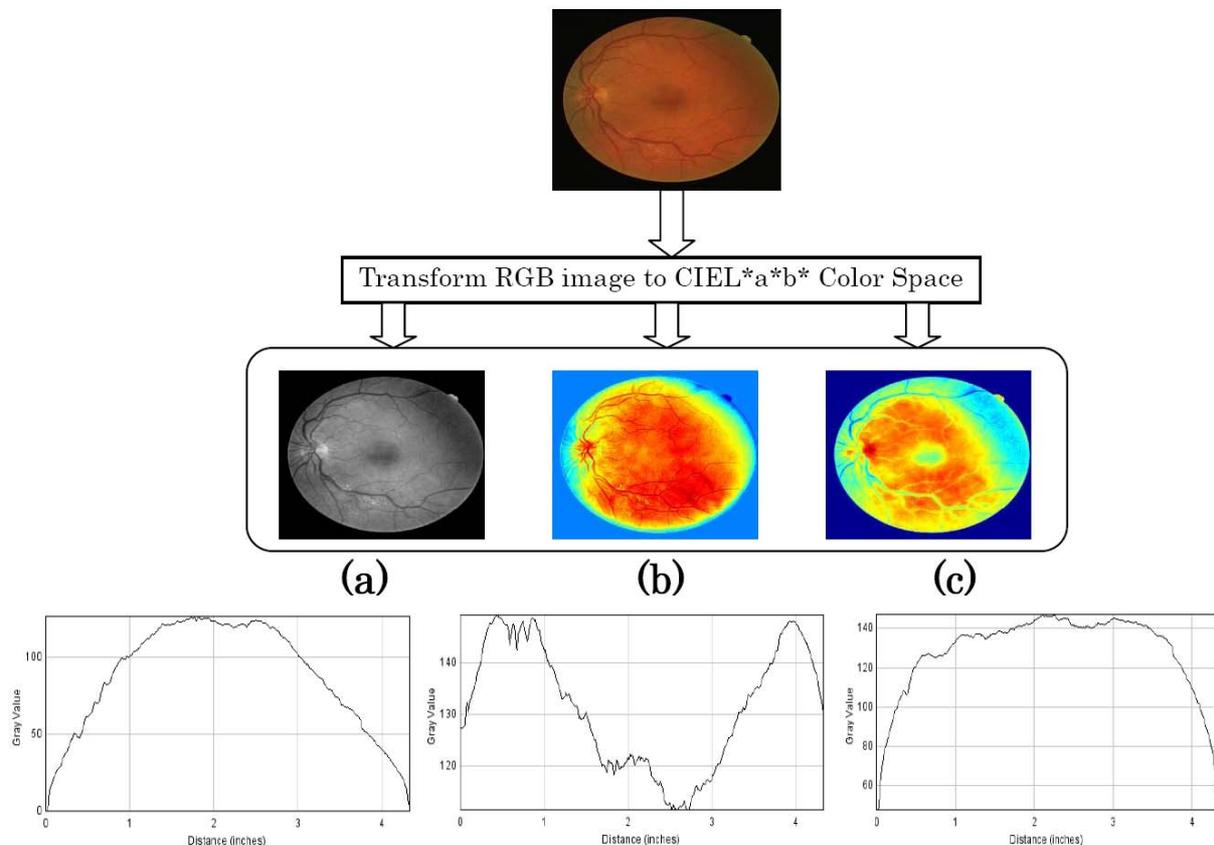


FIGURE 2. The transformation of *sRGB* image to $CIE L^*a^*b^*$ perceptually uniform color space, where (a) shows the luminance image, (b) and (c) represent Chroma components with the corresponding graylevel plots.

as compared with other planes for vessels and background as the plot is shown in Figure 2(a). Contrast may be enhanced using the L^* image but with a nonlinear transform mapping function in a multiresolution analysis (MRA) approach.

4. Discrete Shearlet Transform. The L^* plane of $CIE L^*a^*b^*$ color space is used to correct uneven illumination and to enhance the details while preserving the main characteristics of the images by using the discrete Shearlet transform [16,17] in a multiresolution analysis (MRA) decomposition step.

The OD object in a retinal image has brighter edges than the other background areas and usually it possesses weaker edges than the surrounding area. Similarly, when the blood vessels in the retinal image are wide with strong edges they are easily detected. Meanwhile, the lesions and nerves are hard to identify due to the gray level similarity respect to the background. In the proposed strategy, the algorithm tries to amplify the weak edges so that the thin vessels become more visible and the weak object edges become sharper. Therefore, the proper transform is the one that possesses the edge enhancement capability while introducing no noise in the reconstruction phase. In practice, the shearlets form a tight frame at various scales and directions, and optimally representing the edges of image. With respect to the curvelets and Contourlet as used in [12], it has many fundamental properties of edge enhancement without introducing noise in the reconstruction step. The shearlets are defined on the action of shearing transformations so no generation of noise [16].

In this enhancement study, we have used 4 scales subbands in the frequency domain by using the Laplacian Pyramid transform, which is analyzed by a directional filtering. The empirical results suggested that 4 scales decomposition is sufficient for the color image enhancement. Interested readers may refer to [16,17] for a more detailed information about DST technique. In particular, the algorithm obtains the Shearlet coefficients from the 4 scales of the Laplacian pyramid in frequency division with several shearing filters. In order to enhance the L^* image in the DST domain, the shearing filters with different directions are chosen by using a Meyer wavelet window [16]. Moreover, a non-linear mapping function for post-filtering is performed to further enhance the resulting image.

5. Uneven Illumination Correction and Contrast Enhancement. As it has been already explained, the Shearlet coefficients in the MRA are extracted from the Laplacian Pyramidal representation of the image and used to correct the uneven illumination and enhance the contrast for both gray scale and color retinal images. In order to obtain an image enhancement without generating artifacts an adaptive non-linear mapping function is applied to the generated subbands emphasizing certain features within a certain range. In practice, the OD and CUP areas of retinal-vascular image are brighter than other areas. Therefore, to avoid saturation effect on these areas, the local-influence control function is developed. The aim to introduce this function is to restrict the enhancement step to improve the neighborhood pixels by ignoring these pixels. Subsequently, these transformed components are combined with the other subbands and used in the reconstruction step by means of the inverse discrete Shearlet transform (IDST) to obtain an enhanced luminance component.

Previous to this enhancement step, we have first performed a gamma correction to the high-pass band image on windows of 16×16 pixels size to enhance contrast. Next, for brightness and contrast normalization, the lower pass-band image is enhanced using the nonlinear mapping function. Let lower pass-band image of Laplacian Pyramidal representation be denoted by $C_{(s,d,n,n)}$ in the frequency domain, which is indexed by scale s and direction d of size $n \times n$ pixels. Then, the nonlinear mapping function map of each

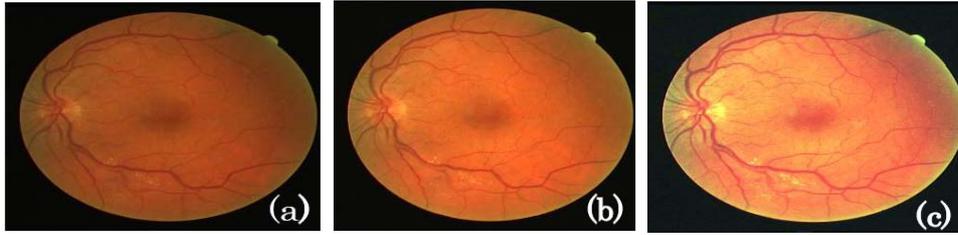


FIGURE 3. Retinal vascular DRIVE image enhancement results for (a) RGB image from datasets, (b) gamma corrected image, and (c) light intensity adjustment of luminance component.

coefficient $G(x, y)$ is defined on $C_{(s,d,n,n)}$ as:

$$G(x, y) = \left\{ \begin{array}{ll} \max \left(\left(\frac{\gamma \sigma_k}{|C_{(s,d,n,n)}(x, y)|} \right)^m, t \right) C_{(s,d,n,n)}(x, y), & \text{if } |C_{(s,d,n,n)}(x, y)| \leq t \sigma_k \\ C_{(s,d,n,n)}(x, y) & \text{otherwise} \end{array} \right\} \quad (3)$$

where γ is the gamma correction value, σ_k is the average intensity variance in $C(x, y)$ subband image of 16×16 window size and t is the threshold value that describes the maximum intensity range condition. The value of t is determined by maximum value of histogram bin in the image. Consequently, the maximum intensity level is maintained by using $G(x, y)$ nonlinear mapping function. However, the *OD* edges and the area within it (cup) are brighter than the other objects in the retinal vascular image. Therefore, we have imposed a local-influence control condition that if the maximum intensity level reaches a value of 1.8, the area remains unaffected by $G(x, y)$ function. Hence, the features are more emphasized and brighter as compared with the surrounding background of each orientation subband components. Next, we performed the inverse *IDST* reconstruction process to get the enhanced luminance L' plane and subsequently the enhanced $L'a*b^*$ image that is converted back to *sRGB* color space for visualization. Figure 3 is visually represented the enhancement results. In this enhancement method, 1.5 value of gamma is used, which is determined by experiments.

6. Results. To test the proposed retinal vascular image enhancement method, we have used three different datasets consisting of total 271 images obtained from DRIVE: 40, STARE: 81 and Private: 150. The accuracy of the proposed method is compared with some state-of-the-art image enhancement methods such as (histogram equalization (HE), HSI (hue, saturation and intensity) color model [10] and Contourlet transform [12]) by using peak signal to noise ratio (PSNR) quality metric. A high PSNR value indicates that the reconstruction is of high quality. The value of PSNR is calculated on each plane of the RGB image that cumulatively describes the image quality as compared with input image.

For performance comparisons to the retinal image enhancement by Contourlet transform [12], first, we have divided into subbands to complete the Laplacian Pyramid (*LP*) method and then the bandpass/detail image is analyzed by a directional filter banks. For the Contourlet transform, we have used five *LP* levels and 32 directions at the finest level. Some of the proposed perceptually-oriented contrast enhancement algorithms results are shown in Figure 4 on the private dataset. The figures show that the contrast and illumination problems are solved without generating artifacts such as saturation and, moreover, the details are preserved.

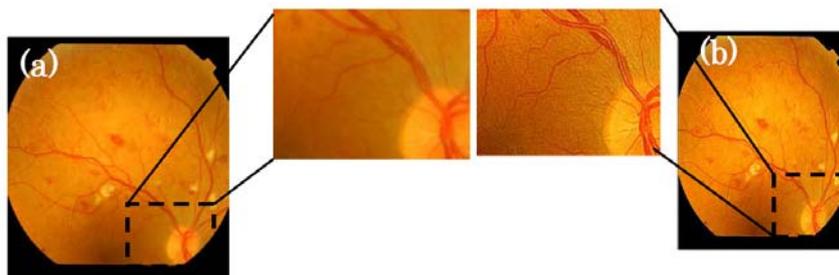


FIGURE 4. The result of color image enhancement with feature-preserving characteristics from the private dataset obtained the Hospital Puerta del Mar (Cádiz, Spain), where (a) is the original image and (b) is the enhanced image by proposed method.

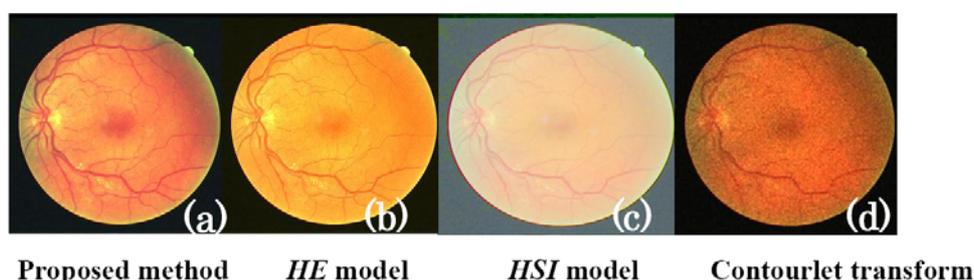


FIGURE 5. Performance comparison for the four different image enhancement methods

TABLE 1. Competitive results obtained from proposed method with other three state-of-the-art methods using PSNR ratio

Proposed method	HE model	HSI model	Contourlet transform
<i>PSNR (R): 9.9223</i>	<i>PSNR (R): 6.0123</i>	<i>PSNR (R): 8.2638</i>	<i>PSNR (R): 8.0498</i>
<i>PSNR (G): 8.3364</i>	<i>PSNR (G): 4.0498</i>	<i>PSNR (G): 1.8353</i>	<i>PSNR (G): 2.2035</i>
<i>SNR (B): 5.2385</i>	<i>PSNR (B): 8.0498</i>	<i>PSNR (B): -3.2552</i>	<i>PSNR (B): 5.6780</i>
Total: 23.4973	Total: 18.1119	Total: 6.8438	Total: 15.9313

The accuracy of our proposed algorithm with the state-of-the-art enhanced methods such as (i) HE model, (ii) HSI model and (iii) Contourlet transform in terms of PSNR is displayed in Figure 5. The quantitative comparisons results are also shown in Table 1. As it can be observed from this table that our proposed algorithm achieves a value of PSNR of 23.5 in total from each red (R: 9.92), green (G: 8.34) and blue (B: 5.24) channels. Figure 5(b), Figure 5(c) and Figure 5(d) are the enhancement results of HE model (total: 18.1, R: 6.01, G: 4.05, B: 8.05), HSI model (total: 6.84, R: 8.26, G: 1.83, B: -3.25) and Contourlet transform (total: 15.90, R: 8.04, G: 2.20, B: 5.68), respectively. The higher PSNR value is obtained by the proposed method followed by the HE, HSI and Contourlet transform algorithms.

It is clear that the uneven illumination is adjusted on image, contrast is improved and features are preserved after using the proposed method. By using this method, a few unrecognizable capillary vessels are easily identified and the edges of the OD area become more apparent as compared with surrounding region. As shown in Figure 5(b), the HE enhancement algorithm disturbs the OD and other areas parts due to the introduction of the standard deviation equation. Moreover, other basic disadvantages also exist in the

HE method when applied to retinal images: i) the absence of some grey levels and non-uniform background/luminosity distribution. This drawback can be easily observed: some parts of the vessels become invisible due to the excessively bright background. Another disadvantage is well-known: histogram equalization strongly amplifies noise. This feature will make the subsequent step (vessel segmentation, microaneurism detection, etc.) hard to complete and even destroy some part of the desired lesion.

The results of retinal image enhancement by HSI model are shown in Figure 5(c). It should be noticed that the local enhancement which aims at normalizing each pixel of the image to zero mean and unit variance also amplifies the noise and make the image strongly brighter. As this figure represents, the edges of blood vessels and nerves of the retinal image are enhanced by this method. Figure 5(a) and Figure 5(d) show the comparison of the discrete shearlet transform (DST) and Contourlet transform enhancement. Our enhancement using DST approach clearly provides better quality results than Contourlet transform technique because of the introduction of the noise factor, which is very hard to amplify during the reconstruction process.

7. Conclusions. A novel color contrast enhancement method is developed with features-preserving characteristics by using a multiscale discrete-shearlet transform (DST), the perceptual uniform color space (CIEL*a*b*) and local-influence control function. The DST coefficients of the luminance image (L^*) has been updated by gamma correction and adaptive non-linear mapping function without affecting other parts of the retinal fundus image using control function. After that the inverse DST is computed to reconstruct the image with the updated coefficients of L^* and this plane is recombined with the corresponding a^* and b^* planes to obtain the enhanced image. This proposed method has been compared with other three methods such as histogram equalization (HE), HSI model and Contourlet-based enhancement by using PSNR image quality measure. The application of this method is tested on retinal images obtained from two publicly available datasets DRIVE: 40 and STARE: 81 and a private one: 150. The experimental results on these datasets indicate that our enhancement method outperforms than other methods, while preserving the main characteristics of the image. This conclusion suggests the idea of introducing this preprocessing step in any CAD tool for early diagnosis of some diseases such as Diabetic Retinopathy. In the future work, the microaneurisms and OD area will be detected and the effect of this algorithm will be noticed.

Acknowledgment. This research work is partially supported by Higher Education Commission (HEC) and COMSATS, Pakistan. The authors also gratefully acknowledge the helpful comments and suggestions of the reviewers, which have improved the presentation.

REFERENCES

- [1] N. G. Congdon, D. S. Friedman and T. Lietman, Important causes of visual impairment in the world today, *JAMA*, vol.290, no.15, pp.2057-2060, 2003.
- [2] Q. Abbas, I. Fondón, S. Jiménez and P. Alemany, Automatic detection of optic disc from retinal fundus images using dynamic programming, *Image Analysis and Recognition Lecture Notes in Computer Science*, vol.7325, pp.416-423, 2012.
- [3] M. Niemeijer, B. V. Ginneken, M. J. Cree, A. Mizutani, G. Quellec et al., Retinopathy online challenge: Automatic detection of microaneurysms in digital color fundus photographs, *IEEE Trans. on Med. Imaging*, vol.29, no.1, pp.185-95, 2010.
- [4] M. U. Akram, S. Khalid and S. A. Khan, Identification and classification of microaneurysms for early detection of diabetic retinopathy, *Pattern Recognition*, vol.46, no.1, pp.107-116, 2013.
- [5] L. Giancardo, F. Meriaudeau, T. P. Karnowski, Y. Li, S. Garg, K. W. Tobin Jr. and E. Chaum, Exudate-based diabetic macular edema detection in fundus images using publicly available datasets, *Medical Image Analysis*, vol.16, no.1, pp.216-226, 2012.

- [6] U. T. V. Nguyen, A. Bhuiyan, L. A. F. Park and K. Ramamohanarao, An effective retinal blood vessel segmentation method using multi-scale line detection, *Pattern Recognition*, vol.46, no.3, pp.703-715, 2013.
- [7] J. Jan, J. Odstrcilik, J. Gazarek and R. Kolar, Retinal image analysis aimed at blood vessel tree segmentation and early detection of neural-layer deterioration, *Computerized Medical Imaging and Graphics*, vol.36, no.6, pp.431-441, 2012.
- [8] M. E. Martinez-Perez, A. D. Hughes, S. A. Thom, A. A. Bharath et al., Segmentation of blood vessels from red-free and fluorescein retinal images, *Medical Image Analysis*, vol.11, no.1, pp.47-61, 2007.
- [9] X. You, Q. Peng, Y. Yuan, Y. Cheung et al., Segmentation of retinal blood vessels using the radial project and semi-supervised approach, *Pattern Recognition*, vol.44, no.10-11, pp.2314-2324, 2011.
- [10] M. D. Saleh and C. Eswaran, An automated decision-support system for non-proliferative diabetic retinopathy disease based on MAs and HAs detection, *Computer Methods and Programs in Biomedicine*, vol.108, no.1, pp.186-196, 2012.
- [11] M. Foracchia, E. Grisana and A. Ruggeri, Luminosity and contrast normalization in retinal images, *Medical Image Analysis*, vol.9, no.3, pp.179-190, 2005.
- [12] P. Feng, Y. Pan, B. Wei et al., Enhancing retinal image by the Contourlet transform, *Pattern Recognition Letters*, vol.28, pp.516-522, 2007.
- [13] E. Grisan, A. Giani, E. Ceseracciu and A. Ruggeri, Model-based illumination correction in retinal images, *Proc. of the 3rd IEEE International Symposium in Biomedical Imaging: Nano to Macro*, pp.984-987, 2006.
- [14] G. D. Joshi and J. Sivaswamy, Colour retinal image enhancement based on domain knowledge, *Proc. of Indian Conf. on Computer Vision, Graphics and Image Processing*, pp.591-598, 2008.
- [15] M. F. Hossain and M. R. Alsharif, Minimum mean brightness error dynamic histogram equalization for brightness preserving image contrast enhancement, *International Journal of Innovative Computing, Information and Control*, vol.5, no.10(A), pp.3249-3260, 2009.
- [16] G. Easley, D. Labate and W. Q. Lim, Sparse directional image representations using the discrete shearlet transform, *Applied and Computational Harmonic Analysis*, vol.25, no.1, pp.25-46, 2008.
- [17] W. Q. Lim, The discrete shearlet transform: A new directional transform and compactly supported shearlet frames, *IEEE Trans. on Image Process*, vol.19, no.5, pp.1166-80, 2010.
- [18] J. Pan, C. Zhang and Q. Guo, Image enhancement based on the Shearlet transform, *ICIC Express Letters*, vol.3, no.3(B), pp.621-626, 2009.
- [19] J. J. Staal, M. D. Abramoff, M. Niemeijer, M. A. Viergever and B. van Ginneken, Ridge based vessel segmentation in color images of the retina, *IEEE Transactions on Medical Imaging*, vol.23, pp.501-509, 2004.
- [20] B. McCormick and M. Goldbaum, STARE = Structured analysis of the retina: Image processing of TV fundus image, *USA-Japan Workshop on Image Processing*, Jet Propulsion Laboratory, Pasadena, CA, 1975.
- [21] P. Green and L. MacDonald, *Colour Engineering, Achieving Device Independent Colour*, John Wiley and Sons, Braishfield, 2002.
- [22] W. D. Niven, *The Scientific Papers of James Clerk Maxwell*, Dover Phoenix Edition, Nueva York, 2003.